Proceedings of IMECE2008
2008 ASME International Mechanical Engineering Congress and Exposition
November 2-6, 2008, Boston, Massachusetts, USA

IMECE2008-67934

TEMPERATURE-DEPENDENT PERMEABILITY OF MICROPOROUS MEMBRANES FOR VAPOR VENTING HEAT EXCHANGERS

Amy M. Marconnet
Department of Mechanical Engineering
Stanford University,
MERL 247 - Microscale Heat Transfer Lab,
Stanford, CA 94305
amymarco@stanford.edu

Milnes P. David
Department of Mechanical Engineering
Stanford University,
MERL 247 - Microscale Heat Transfer Lab,
Stanford, CA 94305
mpdavid@stanford.edu

Anita Rogacs
Dept. of Mechanical Engineering
Stanford University
Stanford, CA

Roger D. Flynn
Dept. of Mechanical Engineering
Stanford University
Stanford, CA

Kenneth E. Goodson
Dept. of Mechanical Engineering
Stanford University
Stanford, CA

ABSTRACT

Improved flow regime stability and lower pressure drop may be possible in two-phase microfluidic heat exchangers through the use of a hydrophobic membrane for phase separation. Past research on vapor-venting heat exchangers showed that membrane mechanical and hydrodynamic properties are crucial for heat exchanger design. However, previous characterizations of hydrophobic membranes were primarily carried out at room temperatures with air or nitrogen, as opposed to liquid water and steam at the elevated operating temperature of the heat exchangers. This work investigates laminated PTFE, unlaminated PTFE, and nylon membranes and quantifies the permeability of the membranes to air and steam. The pressure drop across the membrane as a function of fluid flow rate and temperature characterizes the membrane permeability. This work will facilitate more focused experimental work and predictive modeling on optimizing membrane properties and will help with the development of more effective vapor venting heat exchangers.

INTRODUCTION

Extending the operating range of microfluidic heat exchangers into the two-phase flow regime could dramatically increase the heat removal capacity and efficiency. However, two-phase microfluidic heat exchangers continue to exhibit large pressure drops and instabilities, which decrease system efficiency and increase the effective thermal resistance. Hydrophobic porous membranes allow separation of water vapor from liquid water within the heat exchanger and should improve the performance and flow stability. In our previous work, we found that membrane surface and flow properties at elevated temperatures were crucial in the optimal design of the heat exchangers. However, there are few data available for the permeability of membrane materials with the pore sizes, thicknesses and operating conditions appropriate for this application.

In our previous work, vapor venting heat exchangers were fabricated from copper with integrated porous hydrophobic Teflon membranes. Copper base fluidic channels were machined with parallel channels. Three types of devices were fabricated: non-venting control devices had a glass slide directly to the base; open venting devices had the porous membrane attached to the base with a porous carbon fiber layer for support; and channel venting devices had the porous membrane attached to the base with laser machined vapor channels. Open venting and control devices showed nearly identical thermal and hydrodynamic performance suggesting that membrane was not venting rather acting like solid wall. The channel venting device showed an improvement in thermal resistance, in part due to additional cooling path provided by forced air cooling. These results indicated that mechanical stability and membrane surface properties at elevated temperature are crucial in the optimal design of the heat exchange. For optimal device operation, membranes require high phase selectivity, strength and stiffness, little or no wear or loss in surface properties and high temperature stability [1].

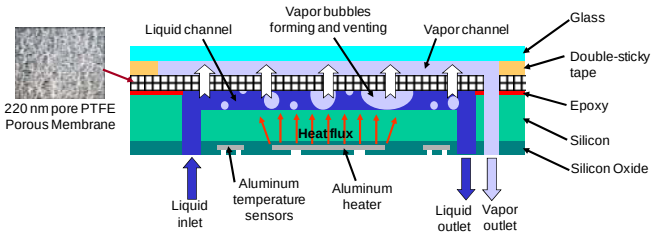

Fig. 1: Vapor venting heat exchanger [10].

Hydrophobic porous membranes have many uses including gas/liquid contactors [2,5], membrane distillation [3,6], filtration [4,7], and proton exchange membrane fuel cells [8]. However, the membranes used in these applications do not necessarily require the high temperature performance needed for our devices and thus the membranes haven't been characterized at the temperature range we require. Drost [2] examined several membranes including commercial membranes such as nylon, polyethersulfone, polyvinylchloride, and PTFE with pore sizes ranging from 0.8 µm to 10 µm with membrane thickness between 50 µm and 160 µm, as well as membranes with engineered straight-through pores from Polyimide (Kapton), polycarbonate, and PDMS. The permeability of the membranes was determined by measuring the mass flux of nitrogen as a function of pressure drop. The permeability of a set of membranes was characterized at room temperature to nitrogen and the membranes with engineered straight-through pores enhanced the mass flux compared to commercial membranes [2]. Martinez et al. [3] developed analytical models of mass flow of water vapor through porous hydrophobic membranes used in membrane distillation, in which, heated water in contact with a porous hydrophobic membrane evaporates though the membrane. The mass flux of air through three porous Teflon membranes was measured as a function of pressure, which allowed calculation the distribution of pore radii in the membrane. From the pore size distribution, the permeability of the membranes to water vapor between 20°C and 80°C was calculated using the analytical model [3]. For our application, we must evaluate the assumption that air and steam interact similarly with porous hydrophobic membranes as well as evaluate the membrane permeability at higher temperatures.

Hydrophobic membranes which have high permeability to steam should selectively allow steam to pass through, but prevent liquid leakage through the membrane. Membrane permeability can be calculated by measuring the pressure drop resulting from flow through a membrane. Commonly a membrane's permeability to steam is assumed to be the same as the permeability to air. The present work measures and compares the permeability of the membrane to steam to the permeability of the membrane to air for the five different membranes listed in Table 1, as well as measuring how the air permeability changes with temperature. From our previous work, the requirements for the membranes to be used in two-phase heat exchanger include native hydrophobicity (high contact angle), high temperature stability, high breakthrough

Table 1: Membranes

Specified Pore size	Teflon	Laminated Teflon	Nylon
0.2 µm	Sterlitech PTU024750	Tefsep by GE F02lP04700	N/A
0.1 µm	Poreflon by Sumitomo HP-010-30	N/A	Magna by GE R01SGH320F5
0.05 µm	Poreflon by Sumitomo UP-005-40rs	N/A	N/A

pressures (pore sizes less than 500 nm based on calculations using the Young-Laplace equation.), and commercial availability. The steam permeability is determined by measuring the pressure drop for steam heated to above 140°C at a fixed flow rate. The air permeability is determined by measuring the pressure drop across a membrane at a flow rate is measured for air set to match the Reynolds number of the steam. To see how the permeability varies with temperature, the pressure drop is recorded while air at the same mass flow rate is heated to between 25°C and 150°C. These experiments are then repeated also with twice the flow rate.

MODELING

Flow of an incompressible fluid through porous media can be modeled as Darcy flow:

$$-\frac{dP}{dx} = \frac{\mu}{K}u = \frac{\mu}{K}\frac{\dot{m}}{\rho A} \tag{1}$$

where P is the pressure, x is the coordinate normal to the membrane, µ is the viscosity of the fluid, u is the average velocity of the flow through the membrane, $\dot{m}$ and ρ are the mass flow rate and density of the fluid, and A is the total area for flow through the membrane. Due to the low Reynolds numbers involved in the flow, we can approximate both the steam and air flow as incompressible. In the Darcy model, the intrinsic permeability K is only dependent on the membrane, not the fluid passing through it [9]. In this model, the viscosity should account for all variations in flow between different fluids. Based on measuring the pressure drop across a porous membrane of thickness, t, at a given mass flow rate, $\dot{m}$, the intrinsic permeability can be calculated through a solution of equation (1) in the form

$$K = \frac{\mu}{\rho}\frac{t}{A}\frac{\dot{m}}{(-\Delta P)} \tag{2}$$

The viscosity and density are fluid properties and the thickness and area are geometric properties of the membrane setup, while the mass flow and the pressure drop can be measured to determine the membrane permeability. The Darcy model is valid for low Reynolds number, where the viscous forces dominate the inertial forces and deviations from the Darcy model occur at high Reynolds numbers where the inertial forces become important. Also, gases at low velocities and pressures may exhibit higher permeabilities than given by the Darcy

model, if the mean free path of the molecule is on the order of the pore size and velocity slip occurs [9].

Martinez et al. [3] instead define a fluid-specific permeability as the mass flux divided by the pressure drop across the membrane:

$$C = \frac{J}{-\Delta P} = \frac{\dot{m}/MA}{-\Delta P} \tag{3}$$

where J is the mass flux and M is the molar mass of the fluid [3]. Comparing the intrinsic permeability to this permeability:

$$C = \frac{\rho}{\mu M t} K \tag{4}$$

Given that the intrinsic permeability, K, is a geometric property, it is evident that C, unlike the K, is dependent on both the membrane and the fluid. For a membrane, comparing C for different fluids or phases allows determination of selectivity. For a given pressure drop across the membrane, the relative values of C determine which fluid or phase will be preferentially transported. For our work, we require a membrane for which the value of C for liquid water is much lower than C for steam at 100°C.

Capillary models describe porous media as networks of small diameter channels and use Navier-Stokes to evaluate the flow. Modeling the porous structure as a set of parallel cylindrical channels, instead of the true tortuous interconnected pore structure, allows the flow to be modeled as Hagen-Poiseuille flow where

$$u_p = \frac{u}{\varepsilon} = -\frac{d^2}{32\mu}\frac{dP}{dx} \tag{5}$$

where u_p is the pore velocity and is related to the average velocity by the porosity, ε, and d is the diameter of an individual pore. In this description, the intrinsic permeability can be calculated to be:

$$K = \frac{\varepsilon d^2}{32} \tag{6}$$

However, few porous media actually agree with the straight-tube assumption. Instead models using networks of both parallel and series connected tubes, though more complex, may more accurately describe porous membranes if the nature of the pore structure could be evaluated [9]. For example, Martinez et al. [3] developed several models for the permeability, C, of water vapor through a porous structure using pore radius distributions. For the case where there is no trapped air in the membrane, so only water vapor exists within in the pores:

$$C = \left[\frac{2}{3}\frac{\pi}{RT}\left(\frac{8RT}{\pi M}\right)^{1/2}\sum_{i=1}^{m}\frac{r(i)^3 n(i)}{qt}\right] + \left[\frac{\pi}{8RT\mu}\sum_{i=1}^{m}\frac{r(i)^4 n(i)}{qt}\right]p_w \tag{7}$$

where R is the gas constant, T is the average membrane temperature, q is the tortuoisity of the porous structure, r(i) is the ith pore radius, n(i) is the number of pores per unit area with pore radius r(i), and p_w is the pressure of the water vapor. Martinez et al. [3] obtained pore radius distributions by measuring Teflon membranes with a Coulter Porometer II and used this model to evaluate the water vapor permeability. Based on the above model, the permeability to water vapor increases with temperature from 20°C to 80°C [3].

EXPERIMENTAL APPARATUS AND METHODS

These experiments characterize the permeability of five membranes including three unlaminated Teflon membranes with pore sizes of 0.2 µm, 0.1 µm, and 0.05 µm, one Teflon membrane with 0.2 µm pores laminated with a polypropylene support layer, and one hydrophobic nylon membrane with 0.1 µm pores. Figure 2 shows the copper fixture built for testing the permeability of membranes. Two 5 mm thick copper pieces are machined with 10 mm diameter, 2.5 mm deep reservoirs. Two 2 mm thick copper stiffener plates with four 2 mm holes limit membrane deflection by reducing the amount of membrane left unsupported for fluid flow. In addition, limiting the area for flow created a measurable pressure drop across the membrane. Membranes are placed between the stiffener plates for characterization. High temperature silicone gaskets between the copper pieces and the membrane prevent leakage and the assembly was bolted together. Thermocouples are fed through the copper fixture to measure the temperature of the fluid just prior to and just after the membrane. In addition for testing the permeability of the steam the temperature of the copper fixture is recorded.

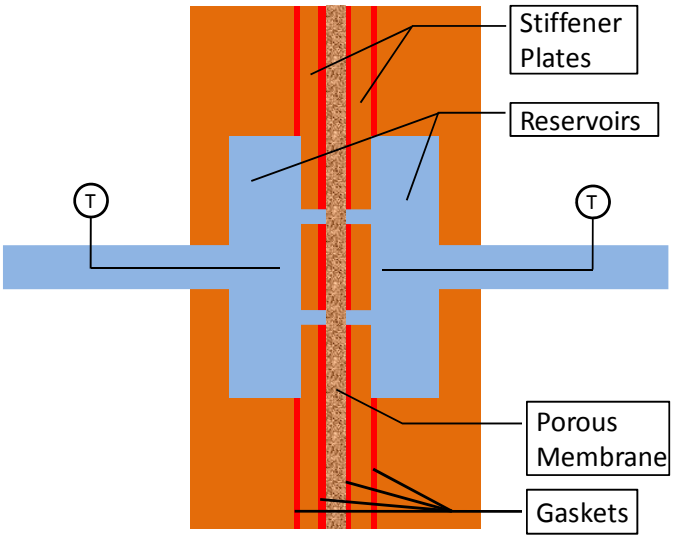

Fig. 2: Permeability Testing Fixture

A peristaltic pump pumps liquid water from a reservoir of deionized water at 0.32 or 0.64 grams/minute through copper tubing wrapped around a cartridge heater to boil the liquid water and form superheated steam. The membrane fixture was heated with a tape heater and insulated. When only steam flows

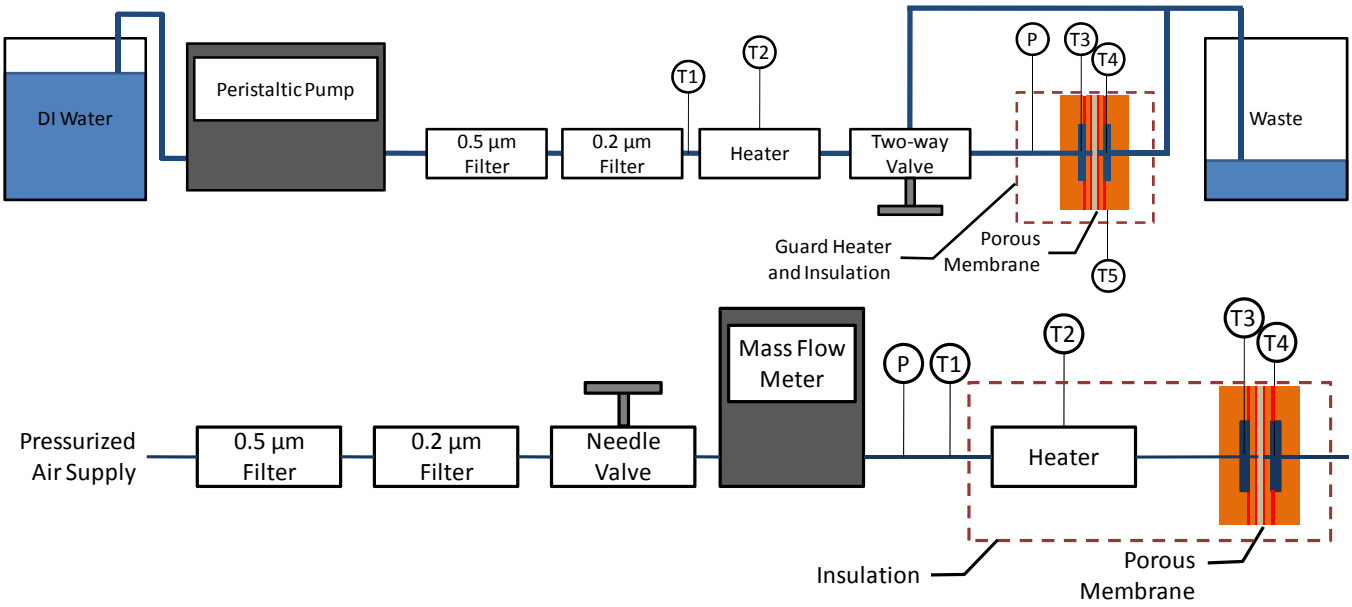

Fig. 3: Experimental set-up. (a) Steam. A two-way valve prior to the membrane fixture allows the fluid to be diverted around the fixture until the steam is superheated and the membrane fixture is heated to 150°C to ensure that when the valve is switched the steam will not condense prior to the membrane. (b) Air.

out of the heater and the membrane fixture reaches 150°C, the two-way valve is switched to flow steam through the membrane. Heating prevents the steam from condensing while passing through the membrane. Figure 3(a) shows the locations of the pressure gage and thermocouples.

Air measurements are performed at 0.4 and 0.8 standard liter per minute (SLPM) to approximate the same value of Re in the steam measurements. The air is heated to more than 100°C and the pressure drop, mass flow rate, and temperatures shown in Figure 3(b) were recorded. A needle valve allows the flow rate to be controlled as the pressure varies with temperature. In addition, at room temperature and the maximum temperature, the pressure drop is measured while varying the flow rate. Figure 4 shows example of the pressure drop, flow rate, and temperature data collected for calculating the air permeabilities.

RESULTS AND DISCUSSION

The intrinsic and fluid-specific permeabilities are calculated using equations (1) and (2) respectively. For the permeability to air, the data is segmented to such that the points

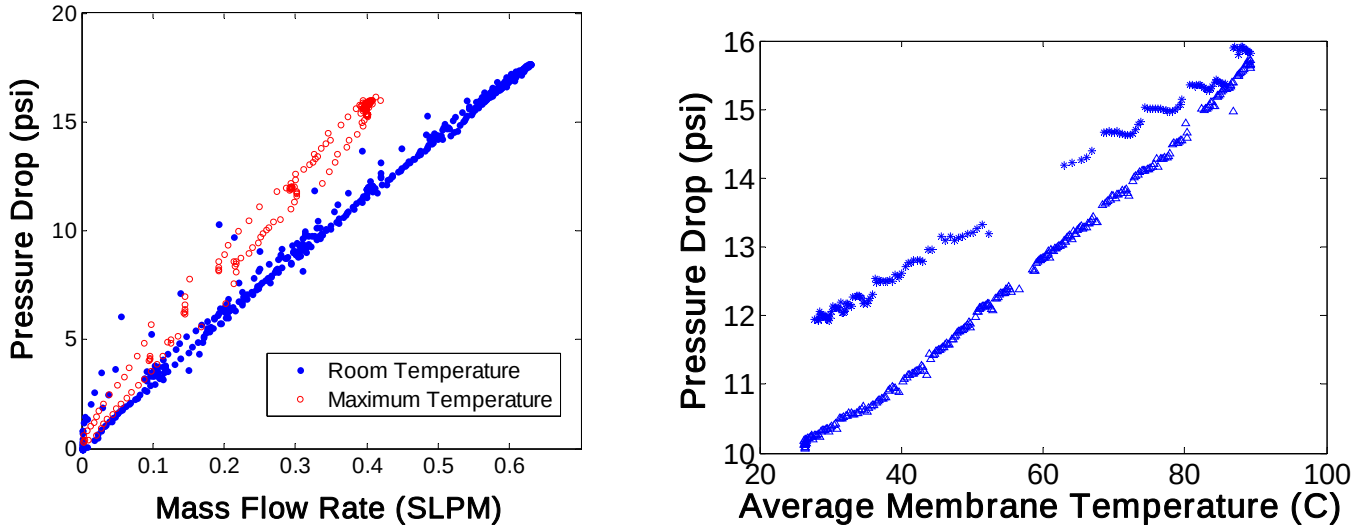

Fig. 4: Left: Pressure Drop vs. Flow Rate for TefSep membrane (Teflon, 0.2 µm pores, laminated) at room temperature (•) and at high temperature (○). Right: Pressure Drop vs. Temperature for the same membrane. The temperature was increased (Δ) and decreased (*) while the flowrate was held constant at 0.4 SLPM and the pressure drop increased as the temperature increased.

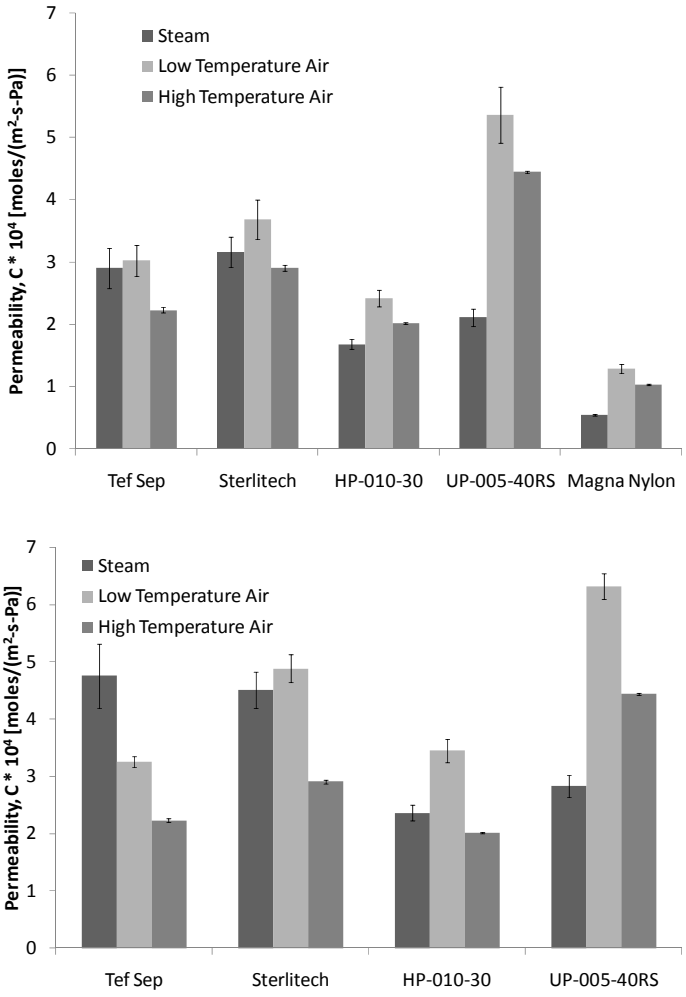

Fig. 5: Fluid-Specific Permeability of Membranes. Top: low flow rate. Bottom: high flow rate.

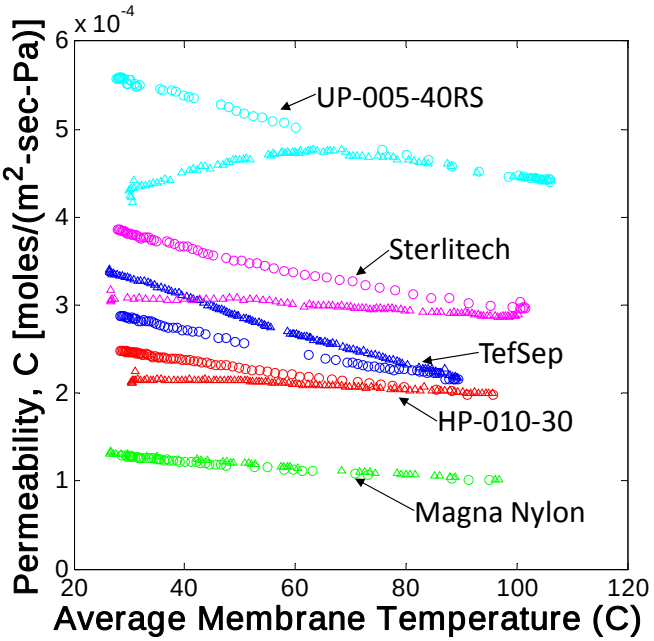

Fig 6: Fluid-Specific Permeability vs. Temperature for Heated Air Flow at 0.40 SLPM. Gaps in data when flow rate drifted from 0.40 SLPM. The variations between heat up (Δ) and cool down ($\circ$) could be due to changes in the fluid properties with temperature and observed changes in intrinsic permeability with temperature. Every 500th data point is shown in this plot.

within 10°C of the maximum temperature achieved and within 0.005 SLPM of the target flow rate are used to calculate the high temperature air permeabilities shown in Figures 5 and 7. The low temperature air permeabilities are calculated from the data points below 35°C and flow rates varied from 0 to 1 SLPM. For the steam permeabilities, data are recorded after the system reaches steady state. Table 2 shows the temperatures and flow rates for the permeabilities in Figures 5 and 7.

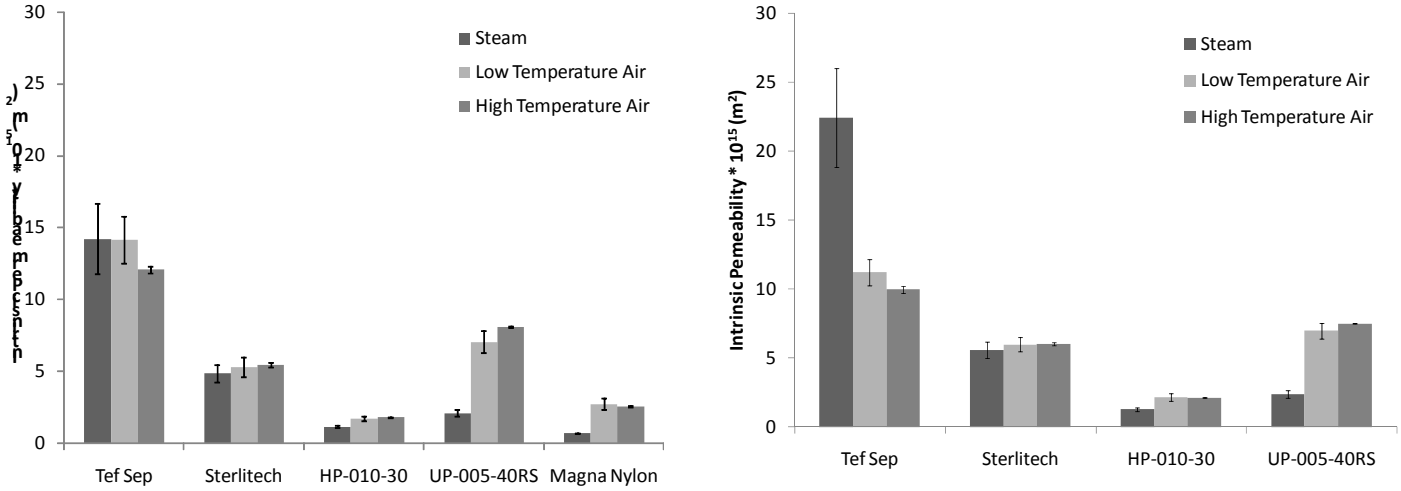

Fig. 7: Intrinsic Permeability of Membranes. Left: low flow rate. Right: high flow rate.

The fluid specific permeability varies with fluid properties and is different for steam versus air as well as the low temperature air and the high temperature air. The changes in permeability from the low temperature air and the high temperature air data for each test can be explained by the changes in fluid properties. For air assuming constant intrinsic permeability, the high temperature and low temperature fluid-specific permeability, C_{high} and C_{low}, vary with the fluid properties as

$$C_{high} = \frac{\rho_{high}}{\rho_{low}} \frac{\mu_{low}}{\mu_{high}} C_{low} \qquad (8)$$

where μ_{high} and μ_{low} are the viscosity, and ρ_{high} and ρ_{low} are the fluid densities all at high temperature and low temperature respectively and are determined from the measured temperature and pressures using lookup tables [12]. At the low flow rate, a temperature increase of approximately 60°C and approximately associated pressure rise should result in approximately a 10-15% reduction in permeability. The low flow rate air data showed a 16-26% decrease in permeability due to the increased temperature. At the high flow rate, the temperature increase of approximately 110°C and associated pressure rise should result in approximately a 18-25% reduction in permeability. The high flow rate air data showed a 24-29% decrease in permeability. The samples showed a larger reduction in permeability than the fluid properties alone would predict. Thus, this data suggests that the intrinsic permeability must change with temperature as well. Figure 6 shows how the fluid-specific permeability changes with temperature for the entire range of temperature measures. Variations in the measured permeability are seen depending on whether the data is taken while the membrane is heating up or cooling down.

The fluid-specific permeability to steam is related to the fluid-specific permeability to air based on fluid properties and the molar mass of the fluid as

$$C_{steam} = \frac{\rho_{steam}}{\rho_{air}} \frac{\mu_{air}}{\mu_{steam}} \frac{M_{air}}{M_{steam}} C_{air} \qquad (9)$$

where the subscripts denote the fluid. Using tabulated properties [11,12], Eq. (9) yields a fluid-specific permeability to steam should that is approximately 5 percent larger than the fluid-specific permeability to low temperature air. The fluid specific permeability to steam is predicted to be 1.7 times the fluid-specific permeability to high temperature air (assuming the air and the steam are at approximately the same pressure). None of the membranes truly followed these relationships. For the HP-010-30, the UP-005-40RS and the Magna Nylon membranes, the fluid-specific permeability to steam was actually much lower than the low temperature fluid-specific permeability to air. The TefSep membrane was inconsistent between the low flow rate test and the high flow rate test, perhaps because for the steam case the laminated polypropylene support failed by the end of the high temperature steam test. For the Sterlitech membrane, the low temperature air permeability and the steam permeability are approximately the same, though the steam permeability is only 1.1 – 1.25

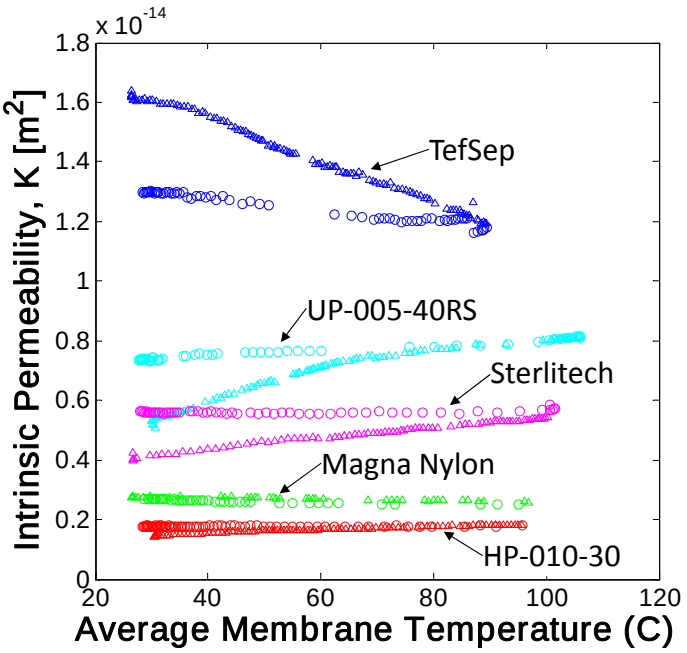

Fig. 8: Intrinsic Permeability vs. Temperature for Heated Air Flow at 0.40 SLPM. Gaps in data when flow rate drifted from 0.40 SLPM. If the flow agrees with the Darcy model, the intrinsic permeability is independent of temperature. For all the membranes that deviate from horizontal lines on the plot above, the major deviation occurs during the heating portion of the experiment (Δ). As the membrane cooled ($\circ$) the permeability was approximately constant. The measured intrinsic permeability during cooling phase remains fairly constant. Although not shown, similar trends were observed for the 0.80 SLPM. Every 500th data point is shown in the plot.

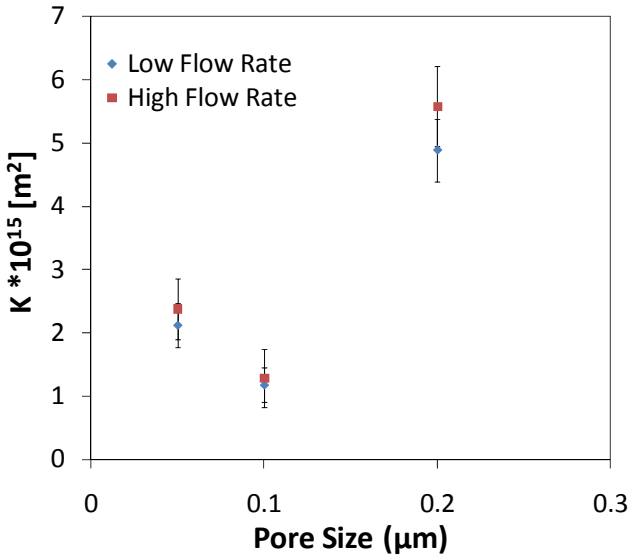

Fig. 9: Intrinsic Permeability vs. Pore Size. Data from measurement of permeability to steam.

times the high temperature air permeability. The differences in the fluid-specific permeability shown experimentally demonstrate that using the air permeability and steam permeability interchangeably or calculating one from the other using equation (9) above is not sufficient for characterizing a membrane.

The intrinsic permeability in the Darcy model is independent of flow rate and fluid properties and should remain constant for all tests. Figure 7 shows, however, that there are differences between air and steam data. The intrinsic permeability is calculated using eq (2) with fluid properties based on the membrane temperature and pressure upstream of the membrane using data tables [11,12]. The low temperature air data are taken at the same range of flow rates and temperatures for both sets of experiments. Any differences in the intrinsic permeability for these data sets would indicate changes in the membrane between the two tests. However, except for the TefSep membrane, the changes in intrinsic permeability for this data set were within the scatter of the data, indicating negligible changes in the membrane between the two data sets. Except for the TefSep membrane, the intrinsic permeability of the individual membranes to steam does not change significantly between the two flow rates measured. The low temperature air data is taken after each heating and cooling cycle. There are differences between the high temperature air data at the two flow rates, however the high temperature air at the low flow rate reached approximately 90°C, while the high temperature air at the high flow rate reached 140°C (the specific temperature at ranges are listed in Table 2). Figure 8 shows variation in intrinsic permeability with temperature for air at 0.40 SLPM. Similar results are seen for air at 0.80 SLPM. There is variation between the measured intrinsic permeability when the membrane is being heated versus when it is cooled. In every case, the permeability changed most during the heating phase of the measurement cycle and remained nearly constant during the cooling phase. The intrinsic permeability varies for the measurements to air and to steam, especially evident in the UP-005-40RS and Magna Nylon membranes. The Sterlitech membrane is the only membrane for which the intrinsic permeability is constant for the steam and air.

Figure 9 shows the intrinsic permeability versus pore size for the three unlaminated Teflon membranes. No clear trend is seen between the permeability and pore size. A membrane with high porosity and small pores may have a larger permeability than a membrane with a low porosity but large pore size. The small pores may each individually have more resistant to flow, however a larger porosity allows more conduits for flow through the membrane. To draw conclusions on the influence of pore size on flow, the effects of porosity and pore size must be separated.

The membranes tested vary from the simple relationship predicted by Darcy's law where the intrinsic permeability is only a property of the membrane. One explanation may be that despite the use of the stiffener plates, some deflection of the porous membranes was seen when the membrane was removed from the fixture. The same membrane is used in the low flow rate dataset and the high flow rate data set. The pressure increases with temperature which causes the membrane to deflect and could change the pore size. Modeling the pores as straight cylinders and using the Hagen-Poiseuille flow given in equation (5), then the intrinsic permeability should be proportional to the pore area or the pore diameter squared as shown in equation (6). Based on the residual deflection after the experiment, the area of the pore may have increased by 50%, which would result in a 50% increase in permeability from the original flat membrane. However, the defection during the experiment was likely larger as the membrane plastically deformed and it is possible it varied from with temperature and flow rate. Increasing the temperature or flow rate both increase the pressure drop across the membrane and result in larger membrane deflection, larger pores, and a higher permeability.

Another explanation for the departure from the Darcy equation is that the temperature at the membrane inlet is 30-50°C greater than at the outlet of the membrane for air when

Table 2: Temperatures and flow rate ranges for fluid used for calculating permeabilities

	TefSep		Sterlitech		HP-010-30		UP-005-40		Magna Nylon		Flow Rates		
	Temperatures		Temperatures		Temperatures		Temperatures		Temperatures		Air		Steam
	min	max	min	max	min	max	min	max	min	max	min	max	-
	[C]	[C]	[C]	[C]	[C]	[C]	[C]	[C]	[C]	[C]	SLPM	SLPM	g/min
Water	146	167	143	174	167	181	157	176	180	185	-	-	0.32
Air -Low Temp	28	35	27	34	28	34	27	34	27	34	0.050	1.000	-
Air -High Temp	79	89	96	106	86	96	96	106	87	97	0.395	0.405	-

	TefSep		Sterlitech		HP-010-30		UP-005-40		Magna Nylon		Flow Rates		
	Temperatures		Temperatures		Temperatures		Temperatures		Temperatures		Air		Steam
	min	max	min	max	min	max	min	max	min	max	min	max	-
	[C]	[C]	[C]	[C]	[C]	[C]	[C]	[C]	[C]	[C]	SLPM	SLPM	g/min
Water	152	179	145	164	152	178	175	181	-	-	-	-	0.64
Air -Low Temp	28	35	26	35	28	35	25	35	-	-	0.050	1.000	-
Air -High Temp	113	123	121	131	122	132	120	130	-	-	0.795	0.805	-

the system is at the maximum temperature. The fluid properties in equation (2) are calculated at the average of the inlet and outlet temperature of the membrane. The temperature difference across the membrane could influence the permeability and that the membrane temperature lags behind the fluid temperature. This is a possible explanation of why at the same temperature the permeability of the membrane while heating is different than the permeability of the same membrane while cooling. There is also a large temperature difference across the membrane for steam, though in some cases it is actually a temperature rise due to the heating of the membrane fixture. The steam data was taken at approximately steady state conditions, not while heating and cooling.

Condensation in the membrane could explain why the steam shows a lower intrinsic permeability than the air when the fluid should not affect the intrinsic permeability. Condensation in the membrane would block pores and prevent the flow of steam through the membrane, as the permeability of the membrane to liquid water is much less than the permeability to steam. Precautions were taken to ensure that the steam did not condense in the membrane. The guard heater keeps the temperature of the membrane fixture sufficiently high so that the steam remains vapor despite the high pressure on the inlet side of the membrane.

CONCLUDING REMARKS

The intrinsic and fluid-specific permeabilities of five different membranes to air and steam were characterized by measuring the pressure drop across the membrane as a function of flow rate and fluid temperature. The measured intrinsic and fluid-specific permeabilities of the membranes varied significantly between air and steam, suggesting the permeability to air should not be used interchangeably with the permeability to steam. Also, the air permeability was measured over a range of temperatures and variation not consistent with the Darcy model was observed. It is possible the deviation is a result of deflection in the membrane during testing or the large temperature difference across the membrane. More testing of the membranes is required to determine the specific cause of the deviation from the Darcy model and to adequately characterize and select the best membrane for selectively venting water vapor. Membranes having high permeability to steam, low leakage, and minimal changes in permeability while in use are ideal for two-phase vapor venting heat exchangers. Based on these requirements, the UP-005-40 and the nylon membranes look promising for the heat exchanger applications.

ACKNOWLEDGMENTS

This material is based upon work supported under a National Science Foundation Graduate Research Fellowship and Stanford Graduate Fellowships. The authors would like to acknowledge the support of the MARCO Interconnect Focus Center, one of five research centers funded under the Focus Center Research Program, a Semiconductor Research Corporation program. We are grateful to Sumitomo Electric Interconnect Products, Inc. for donating several of the membranes tested in this study.

REFERENCES

[1] David, M.P., Marconnet, A., and Goodson, K.E., "Hydrodynamic and Thermal Performance of a Copper Vapor-Venting Heat Exchanger," ASME-ICNMM 08, Darmstadt, Germany, June 23-25, 2008, Paper #62269 (IN REVIEW).

[2] Drost, M.K. Enhancement of Heat and Mass Transfer in Mechanically-Constrained Ultra-Thin Films (DE-FC36-01GO11049). U.S. Department of Energy. Golden, CO (2004).

[3] Martinez, L. et al. "Characterisation of three hydrophobic porous membranes used in membrane distillation: Modelling and evaluation of the water vapour permeabilities." J. Membr. Sci. 203 (2002) 15-27.

[4] Evans, P.J. et al. "The influence of hydrophobicity, roughness and charge upon ultrafiltration membranes for black tea liquor clarification." J. Membr. Sci. (2008), doi:10.1016/j.memsci.2008.01.010

[5] Albrecht, W. et al., "Selection of microporous hydrophobic membranes for use in gas/liquid contactors: An experimental approach." J. Membr. Sci. 263 (2005) 66-76.

[6] Khayet, M., Mengual, J.I., and Matsuura, T., "Porous hydrophobic/hydrophilic composite membranes. Application in desalination using direct contact membrane distillation." J. Membr. Sci. 252 (2005) 101-113.

[7] Boussu, K. et al., "Relation between membrane characteristics and performance in nanofiltration." J. Membr. Sci. 310 (2008) 51-65.

[8] Lee, W-k. et al., "Characterization of Permeability Changes and Hydrophobic Nature of GDL, and Correlation with PEMFC Performance." Fuel Cell Seminar, 2004.

[9] Kaviany, M. Principles of Heat Transfer in Porous Media. New York: Springer, 1995.

[10] David, M.P. et al., "A Vapor-venting, micromachined heat exchanger for electronics cooling", Proceedings of 2007 ASME International Mechanical Engineering Congress and Exposition, Seattle, Washington, November 11-15 2007.

[11] Holmgren, M. "XSteam: Water and steam properties according to IAPWS IF-97." <http://www.x-eng.com /XSteam_Matlab.htm>.

[12] Billig, S. "AirProp: Interpolates thermodynamic air properties according to Eckert & Drake, Analysis of Heat and Mass Transfer." < http://www.mathworks.com/ matlabcentral/fileexchange/loadFile.do?objectId=5165>.